Holzforschung, Vol. 63, pp. 168–180, 2009 • Copyright © by Walter de Gruyter • Berlin • New York. DOI 10.1515/HF.2009.017

Fracture toughness, chip types and the mechanics of cutting wood. A review

COST Action E35 2004–2008: Wood machining – micromechanics and fracture

David J. Wyeth[1], Giacomo Goli[2] and Anthony G. Atkins[1,*]

[1] Department of Engineering, University of Reading, Reading, UK

[2] Dipartimento di Scienze e Tecnologie Ambientali Forestali, Università di Firenze, Firenze, Italy

*Corresponding author.
Department of Engineering, University of Reading, Reading RG6 6AY, UK
E-mail: a.g.atkins@reading.ac.uk

Abstract

Historical studies for predicting cutting forces in wood processing are based on the Piispanen/Ernst-Merchant theory employed in metal cutting where the offcut/chip is formed in shear. This analysis has been recently improved to include significant work of surface separation and formation (i.e., the fracture toughness of the workpiece, as well as the shear yield stress and friction). The new theory is applied here to wood cutting experiments. It is well known that chip formation and surface damage depend on grain orientation and chip thickness, but experiments reveal that chip formation alters with cutting speed as well. During the COST E35 action a series of experiments and special devices to orthogonally cut wood at high and low speed have been developed. In this paper, an overview of the cutting devices and the main results are given.

Keywords: different grain orientation; fracture toughness; machining; speed effects; types of chip; wood, cutting.

Introduction and background

Studies to understand and model wood cutting have been performed by several authors over the years. In many cases empirical formulae have been derived and these will be discussed in the section of this paper dealing with cutting forces. The first systematic studies of cutting forces with different grain orientations and the study of the different chip types and formation started in the 1950s and 1960s with the work of Kivimaa (1952), Franz (1958) and McKenzie (1961). From these investigations two separate chip classifications for wood cutting were developed, depending on the grain orientation. Franz (1958) classified chips formed at 0° grain orientation (in line with the direction of cutting), and McKenzie (1961) classified chips formed with a grain orientated 90° to the direction of cutting (this classification is really more related to the subsurface damage than the chip type). Because wood is usually cut in 90–00 and 90–90 cutting orientations, researchers have concentrated their efforts in the analysis and description of these two cutting situations.

Fewer studies have looked at processing with different grain orientations. Studies, when processing with different grain orientations, have been carried on in recent times by Stewart (1971, 1983) who analysed the general behaviour of the cutting forces for wood when orthogonally cut at low speed and computed the cutting friction coefficient. Cyra and Tanaka (2000) described the general macroscopic appearance of the chips when routing with different grain orientations. The final surface condition, when processing with different grain orientations, has been described by Goli et al. (2002). Recently, Costes et al. (2004) have measured the cutting forces in a turning operation of a wood sample, whereby cutting occurred over all the grain orientations. The subject of the interaction between the cutting edge and wood grain was investigated during the COST E35 action by the University of Florence from the start of the programme and, later, in cooperation with the University of Reading. The main purpose of the research was:

- the measurement of the cutting forces during an orthogonal cutting process with different fixed grain orientations;
- to study if a positive intercept is observed in wood cutting when plotting cutting forces versus depth of cut (DoC);
- apply the Atkins (2003) cutting theory to the already known, described and documented cases;
- describe in detail the chip formation when machining with different grain orientations in order to provide fundamental information for the modelling of cutting;
- perform tests at different cutting speeds in order to understand the role of the cutting speed when machining wood;
- implement the chip classifications already existing or develop new chip classifications for the wood cutting process.

In order to achieve these goals, several different experiments have been conducted and specific equipment has been developed.

In this paper, being a report of the activity performed during the COST E35 action, the equipment will be described as well as some of the more significant results. Due to space restrictions in some cases, it will be impossible to explain everything in great detail but some of the outcomes from the activity performed during the COST E35 action have already been published. Topics

concern (1) analysis of the mechanical interactions between wood and tool and the consequential defects appearing on the surface when processing with different grain orientations (Goli et al. 2002, 2004; Goli and Uzielli 2004); (2) surface formation processes when cutting with high and low speeds (Goli et al. 2005, 2006, 2007a,b); and (3) friction between the chip and the tool rake face (Wyeth et al. 2007). Other papers are in preparation.

Materials and methods

Linear cutting was chosen as the test method to understand what happens during processing wood. Two low speed cutting rigs (LSCRs) for orthogonal cutting have been developed, one at the University of Florence, the other at the University of Reading, to measure cutting forces precisely, to clearly observe their evolution during the cut and to observe the formation of chips. At low cutting speeds dynamic vibrational processes are not encountered, and since the collection of chips is much easier because they are not projected away or completely fragmented, chip formation can be easily studied. The study of chip formation is a fundamental factor in understanding what occurs during the cutting process.

Low speed cutting rigs

The LSCRs developed in Florence uses a hydraulic universal testing machine as the drive mechanism. The machine drives a platform located, by means of linear bearings, on four guides (Figure 1b). The velocity of the platform was set to 5 mm s^{-1}. The tool holder was mounted on the platform, whereby the cutting blade was clamped. The cutting blade was a conventional commercial tungsten carbide insert manufactured by Leitz, part number TM 405-0. The geometry of the blade was 55° wedge, 20° rake angle and 15° clearance. Beneath the platform the sample to be cut was mounted on a Kistler® load cell and fixed into position using a clamp mechanism. The samples were pre-prepared to specific dimensions and grain orientations using a precision saw; this ensured that the samples were both parallel and had a good surface finish.

At the University of Reading, an instrumented sledge microtome was developed with which the forces were measured by the use of an extended octagonal strain-gauged load cell, and a uniform tool speed was achieved by driving the specimen with a pneumatic/hydraulic system (Figure 1a). The device was designed so that the blade (having an included wedge angle of 27°) could be tilted, which allowed varying rake angles to be achieved.

For both the machines, because of the low cutting speeds, conventional cameras set in sequential mode, or video cameras, were used to film the cutting process. Images were also taken of the surface of the samples after cutting.

High speed cutting rig

The high speed cutting rig (HSCR) was designed to replicate the cutting geometry of the LSCR of the University of Florence, so that the role of the cutting velocity on the chip formation process could be studied. The high speed device employed a split Hopkinson Bar system (HBS) to drive the cutting tool contained within a specially-designed cutting rig (Figure 1c). The rig consisted of a base which housed a precision-ground cutting shaft that enabled smooth travel through two brass bushes. The motion was transferred to the sliding cutting shaft by the impact of an input bar, propelled at high velocity by the pressure system of the HBS.

A tungsten carbide insert was clamped into a slot in the cutting shaft; this achieved a rake angle of 20°. The insert was the same type as fitted to the University of Florence cutting rig. A larger diameter head was bolted to the end of the shaft, which stopped the shaft after the cutting had been completed. A collar of plasticine® was used to absorb the excess kinetic energy after the cut was completed. Without the collar, the shaft was found to rebound, causing the carbide insert to damage the newly formed surface of the samples. A key fitted to one of the bushes aligned the shaft, which also prevented any rotation of the tool during cutting. The duration of the cutting process, at a cutting velocity of 8 m s^{-1} (the velocity at which most of the tests were performed), was 2.5 ms. To capture the cutting process visually, a Photo-sonics Phantom V7 monochrome high speed camera fitted with a Nikon 24–85 mm F2.8 macro zoom lens was utilis-

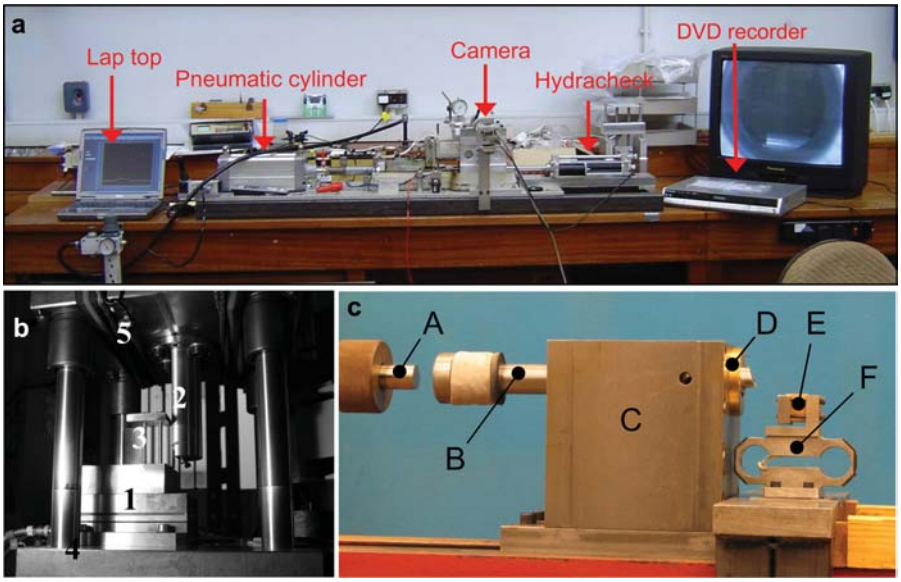

Figure 1 Various apparatus developed in the course of the COST E35 action. (a) Low speed cutting rig (LSCR) (University of Reading). (b) The LSCR apparatus (University of Florence): (1) the dynamometric platform, (2) the tool holder and the tool, (3) the specimen, (4) the lower plate, and (5) the upper plate (image from Goli et al. 2005). (c) High speed cutting rig (HSCR) (University of Reading): (A) input bar, (B) cutting shaft, (C) housing, (D) bush, (E) sample, (F) load cell.

ed. While the camera is capable of recording up to 160 000 frames per second, such a high capture rate resulted in a low image resolution, and clear images were obtained with a capture rate of approximately 15 000 frames per second, giving an image resolution of 512×176 pixels. An exposure time of 40 μs was used and lighting was provided by 2 kW halogen lights. The output of the load cell was recorded using a two-channel AD device connected to a PC with a sampling rate of 100 kHz. Once the cut was performed the sample was removed from the clamp mechanism and saved along with the chip, although some chips were so severely fragmented this was not possible.

Samples tested and sample positioning

Samples of dry Douglas fir were processed at both low and high cutting speeds, employing identical depths of cut and similar tools. The average moisture content (MC) for Douglas fir for the low speed cuts was measured at 9.6%, while for the high speed cuts it was found to be 11.1%, a ΔMC of 1.5% within the two tests. The selected boards were defect-free and had straight grain. The samples were cut as near as possible inside the same board to minimise the wood variability (Figure 2a).

The samples were tangentially cut and orientated so that the surface to be cut with 0° of grain orientation was the radial face (Figure 2b,c). This ensured homogeneous cutting allowing earlywood and latewood to be cut simultaneously. The cut face had dimensions of 14 mm wide and 20 mm long. Samples were machined to obtain a series of grain orientations, achieving a range from 0° (along the grain) to 90° (across the grain) both positive (with the grain) and negative (against the grain). The orientations at +90 and -90, and +0 and -0, were the same samples cut in opposite directions. DoC of 0.1, 0.2, 0.4 and 0.6 mm were made depending on the cutting device, and for each DoC several grain orientations were investigated. Detailed information concerning the setup used in the different devices is shown in Table 1.

The DoC was achieved using dead stops located on a datum face of the sample clamp mechanism. The dead stops were necessary because the reference surface could not be created in the device itself. The reference surface was created by a precision saw in Florence, and by means of a router in Reading

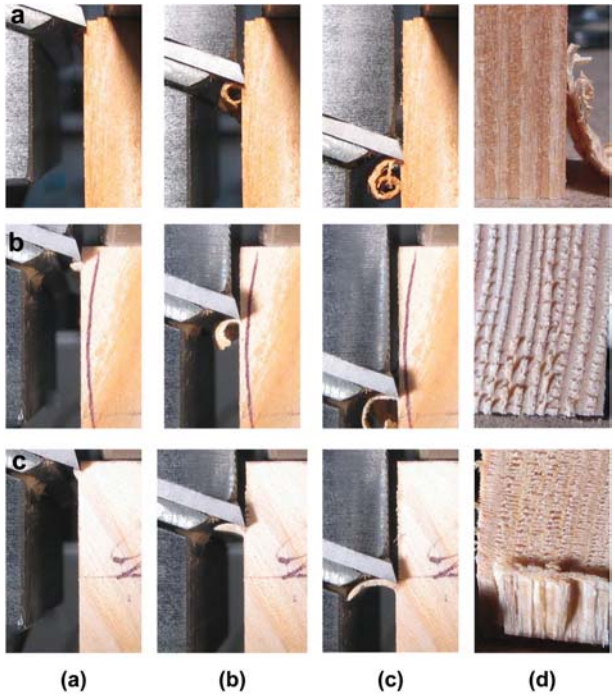

Figure 3 Sequences of processing tangential specimens of Douglas fir. In all cases, (d) illustrates the cut samples surface finish with a 0.6-mm DoC and a cutting speed of 5 mm s^{-1} (all images modified from Goli et al. 2005). (a) Douglas fir processed along the grain, (b) Douglas fir processed 30° with the grain, and (c) Douglas fir processed 30° against the grain.

while a very low feed speed was applied. The specimen was mounted inside the cutting device only after this preparation step. The actual DoC was checked by image analysis software with the stills captured by the camera in the low cutting speed tests; a measure feature within the Phantom Ph606 software was applied together with the high speed camera. In some cases, the chips were weighed to estimate the DoC.

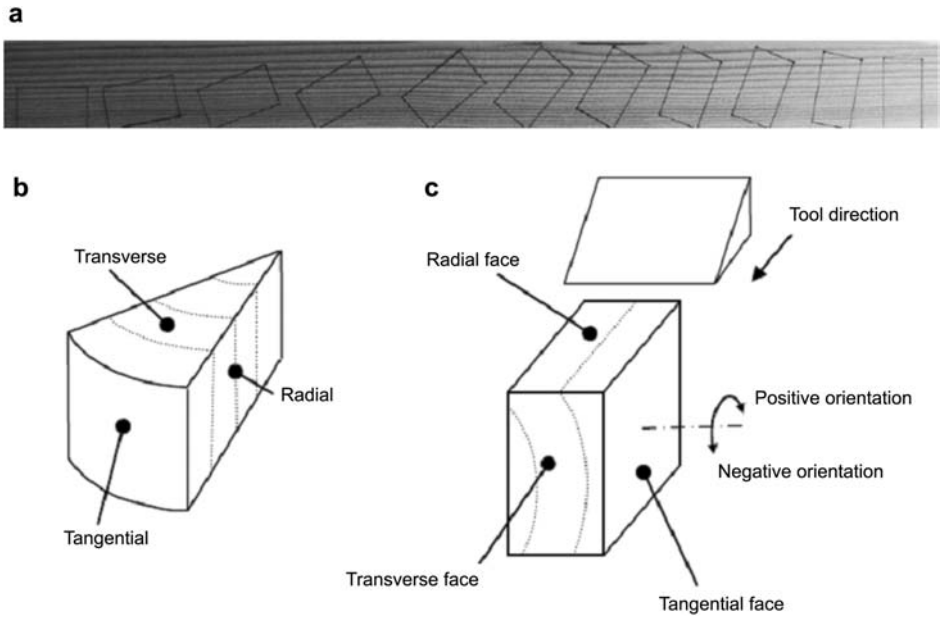

Figure 2 Test sample orientation. (a) One of the boards used to cut the samples with a complete sample series marked on before being cut. Every specimen has an increased grain angle of 10° (image from Goli et al. 2005). (b) Notation of orientations relative to log. (c) Sample orientation and grain angle notation.

Table 1 General scheme of the tests performed on the LSCR and on the HSCR.

Characteristic	LSCR Florence	LSCR Reading	HSCR
Rake angle	20°	60°	20
Wedge angle	55°	27°	55°
Cutting speed	5 mm s^{-1}	13 mm s^{-1}	8 m s^{-1}
Cutting length	20 mm	20 mm	20 mm
Sample width	14 mm	14 mm	14 mm
Cut duration	4 s	2 s	2.5×10^{-3} s
Blade material	Tungsten carbide	High speed steel	Tungsten carbide
Load cell	Tri-axial Kistler piezoelectric	Extended octagonal strain gauge load cell	Extended octagonal strain gauge load cell
Species machined	Douglas fir Azobè, Beech	Douglas fir	Douglas fir
Douglas fir MC	9.6%	11.1%	11.1%
Douglas fir machined depths	0.1, 0.2, 0.4, 0.6 mm	0.1, 0.4 mm	0.2, 0.4, 0.6 mm
Beech machined depths	0.6	/	/
Azobè machined depths	0.6	/	/
Grain orientations machined	-90, -60, -30, 0, 30, 60, 90	-90, -60, -30, 0, 30, 60, 90	-90, -80, -70, -60, -50, -40, -30, -20, -10, 0, 10, 20, 30, 40, 50, 60, 70, 80, 90
Number of repetitions per test	2/3	1	1
Surface cut	Radial and tangential	Radial	Radial
Total number of cuts performed	144	20	75
Sample positioning	Dead stop	Ratchet mechanism	Dead stop
Cutting sequence images	Sequential stills with a digital camera	Video camera	High speed camera

When processing against the grain, the surfaces of the samples were usually destroyed and fractures were found to have propagated deep under the surface. In such cases, the specimens could not be re-cut for a repetition test and a new sample had to be tested; this reduced the number of repetitions that could be performed owing to the limited number of samples available.

Eight or nine LSCR tests and four or five HSCR tests were performed each day. The general scheme of the test is summarised in Table 1.

Experimental results

Low speed cutting

The LSCR developed in Florence worked very effectively. Great care was taken to obtain the desired DoC. The creation of the reference surface on samples was comparatively easy for cutting along the straight grain, but was more difficult when machining with and against the grain. The precision saw used for this purpose was found to be very effective. Figure 3a shows chip formation along the grain with a DoC of 0.6 mm.

The cutting forces could also reveal what occurs during the cutting process. In fact, the fluctuating force plot shown in Figure 4a was typically found when the Franz type I chip (split and bend, explained in detail later) was formed.

Processing with a 0.1-mm DoC results in the formation of a shear plane (Franz type II) chip formation process, this consequently results in almost constant cutting forces being obtained, as shown in Figure 4b.

Processing with the grain (Figure 3b) and against the grain (Figure 3c) results in more complex phenomena which changed with DoC, where transverse compression, fibre bending and shear along the grain have a complicated influence on chip formation in a mixed mode that is rather difficult to predict. As the analysis of this data is still ongoing, it is anticipated that these results will be submitted for future publication.

The cutting forces (Figure 4c, d) behave differently when processing with the grain or against the grain, compared with machining along the grain. An important observation is the progressive increase of the cutting forces instead of attaining the maximum force value immediately after cutting initiates.

The force magnitude clearly shows (Figure 4), even with the same DoC, how processing against the grain requires significantly more force than for the other orientations.

Figure 5 illustrates the cutting forces for a 0.6 mm DoC superimposed on the appearance of the surface obtained after processing Douglas fir 70° against the grain. The link between force fluctuations during the cut, and features on the cut surface, are clearly evident.

By plotting the cutting forces (F_c) and the normal forces (F_n) vs. the grain orientation all at the same DoC (as in Figure 6), the force relation with the grain orientation can be clearly observed. The forces plotted in the graph have been computed per mm of sample width. The error bars represent the variability of the force within the steady state region. Most of these data were obtained from averaging more than one data set, repetition cuts were only performed where the cutting process was unclear.

High speed cutting

High speed cuts (8 m s^{-1}) recorded with the HSCR equipment were found to be very effective and the system worked very well. In particular:

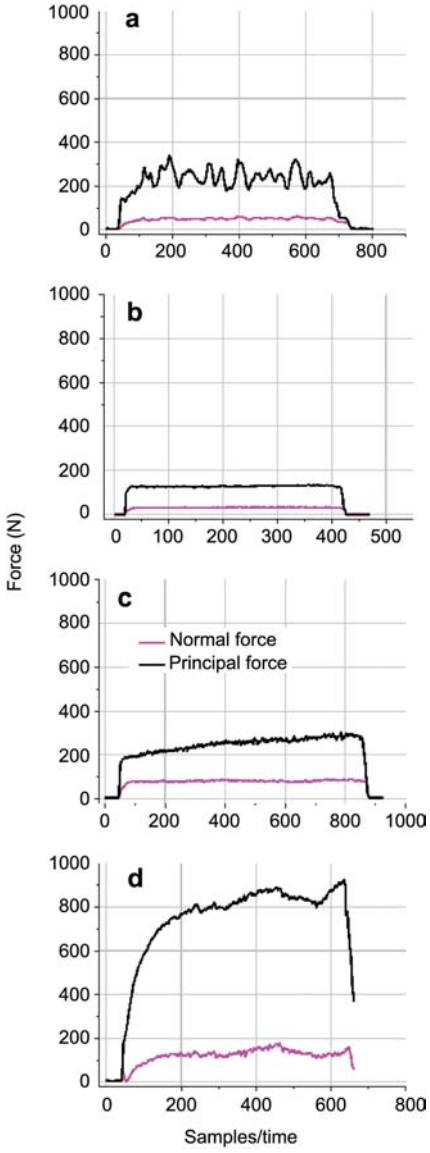

Figure 4 Cutting force plots for processing tangential specimens of Douglas fir with LSCR. (a) Along the grain with 0.6 mm DoC (image from Goli et al. 2005), (b) along the grain with 0.1 mm DoC, (c) 30° with the grain, and (d) 30° against the grain both with 0.6 mm DoC (image from Goli et al. 2005).

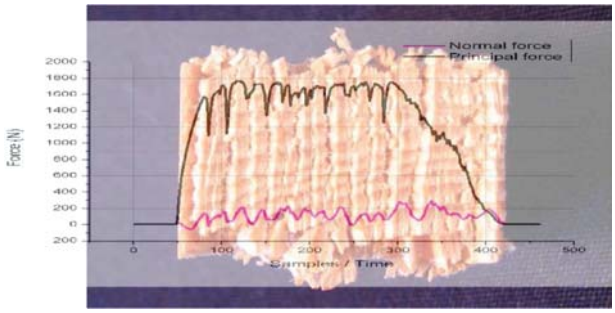

Figure 5 Surface and cutting forces processing a tangential specimen of Douglas fir 70° against the grain with a 0.6-mm DoC with LSCR (image from Goli et al. 2005).

- no deceleration during the cut was observed by the data obtained from the high speed camera, so the cutting speed can be assumed to be constant;
- the cutting path was very linear and consequently the DoC was constant along the whole cutting path;
- the high speed camera enabled effective viewing of the processes involved during the cut;
- the mounting of the load cell on a stand independent of the system eliminated noise from the operation of the system.

Different types of chip formed at the same DoC (0.2 mm) in Douglas fir, but at different grain orientations, were observed (Figure 7).

Measurement of cutting forces under quasi-static conditions posed no problems, but difficulties were encountered in the high speed tests. The cutting force traces shown in Figure 8 are for machining a 0° grain orientation Douglas fir specimen with a 0.2-mm DoC. The results are typical of unfiltered force signals obtained at high speeds with other DoC. While it can be seen in Figure 8 that minimal noise was recorded prior to cutting owing to the sample holder being mechanically detached from the HBS, it is clear that the impact of the blade on the sample excited the force dynamometer measurement system causing it to vibrate at its natural frequency both during the cut and for some time afterwards.

Although there must be uncertainty about the precise values of cutting force in these circumstances, it was decided to plot the first peaks in force in order to observe general trends, as it was considered that the value of these peaks was mainly determined by the cutting forces. Figure 9 depicts the way in which initial peak forces vary with grain orientation for two DoC (0.2 and 0.6 mm) in Douglas fir. It is noteworthy that the general trends of the peak dynamic loads are similar to those obtained when processing at low speeds with the LSCR.

However, even though the cutting geometry of the HSCR and LSCR are the same, the peak forces (F_n) perpendicular to the cutting direction are negative in high speed tests as opposed to positive at low speeds, indicating that at high speed the tool is lifted up during cutting, but at low speed the tool is pressed down when cutting. Why the increase of cutting speed causes this change, and the conditions under which the change occurs, requires further investigation.

Work is continuing to model the HSCR behaviour with the aim of deriving the cutting force behaviour during the whole cut by the implementation of a transfer function. Other models to obtain approximate cutting forces have already been implemented and will be discussed in specific publications under preparation.

Unclassified chip formation processes

A chip, previously not classified within chip types found in orthogonal cutting, has been observed at some grain orientations when processing with the grain at both low and high speed. It occurred when cutting with the grain between 10° and 50–60°. As shown in Figure 10a, it is formed by compression across the grain and shear parallel to the grain. It is similar to chips formed by a disc chipper as described by McLauchlan and Lapointe (1979), but in that case cutting was against an anvil which is completely unlike our orthogonal cutting arrangement.

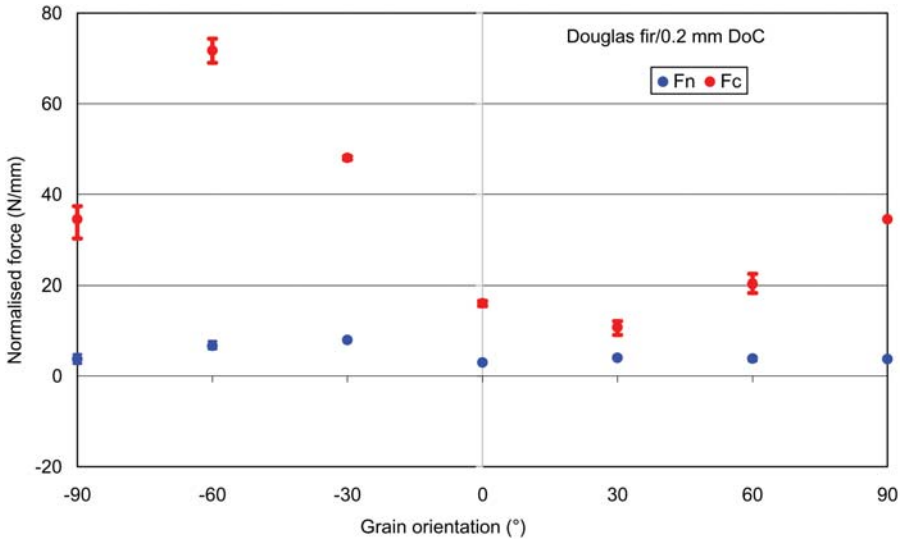

Figure 6 Cutting force (F_c) and normal force (F_n) vs. grain orientation processing radial specimens of Douglas fir with the grain and against the grain with 0.2 mm DoC using LSCR.

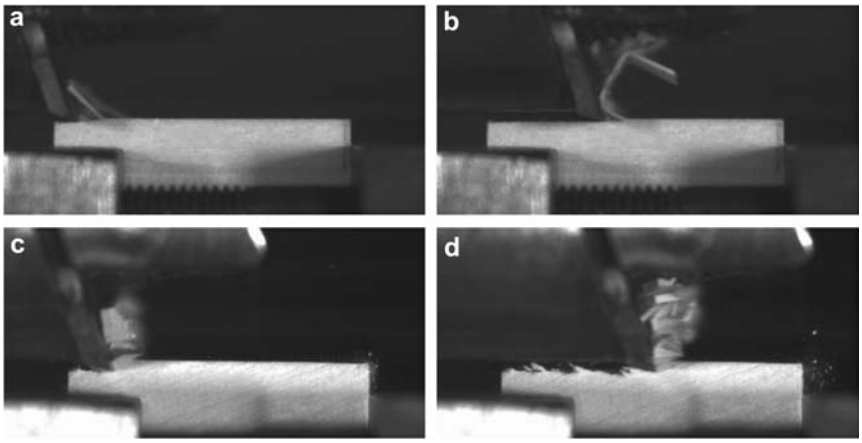

Figure 7 (a, b) Cutting sequence of Douglas fir with 0° of grain orientation. (c, d) Cutting sequence of Douglas fir with 20° of grain orientation (0.2 mm DoC, cut at 8 m s^{-1}).

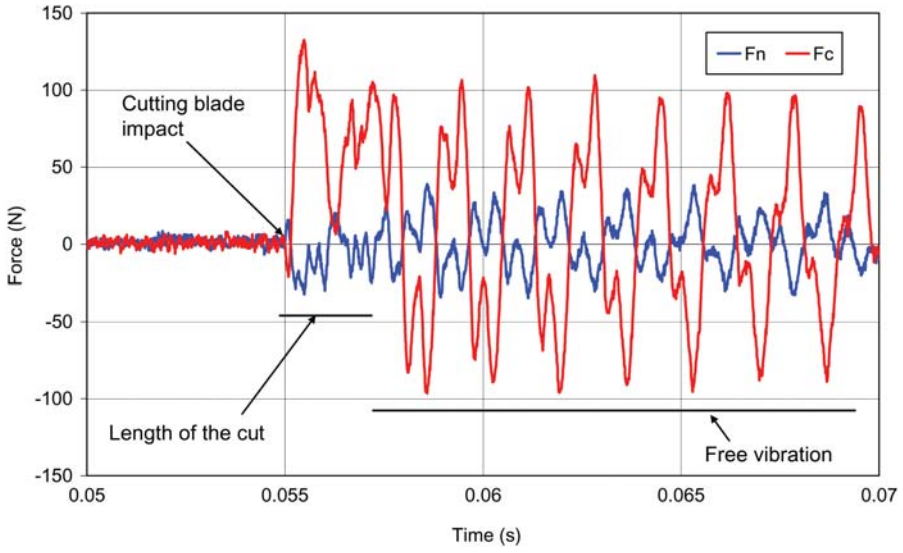

Figure 8 Cutting signal obtained machining Douglas fir 0° of grain orientation 0.2 mm DoC with the HSCR.

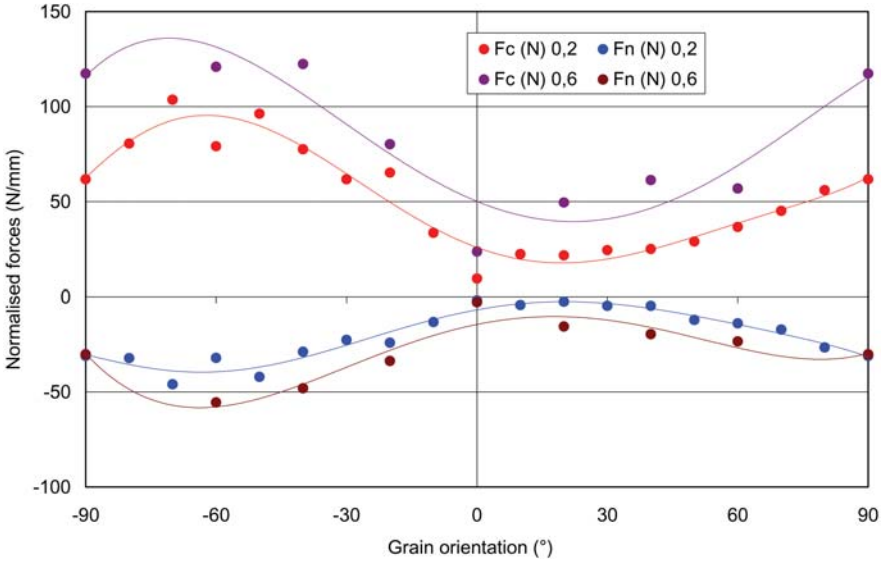

Figure 9 Plot of the values of the first peak after the impact, cutting with the HSCR.

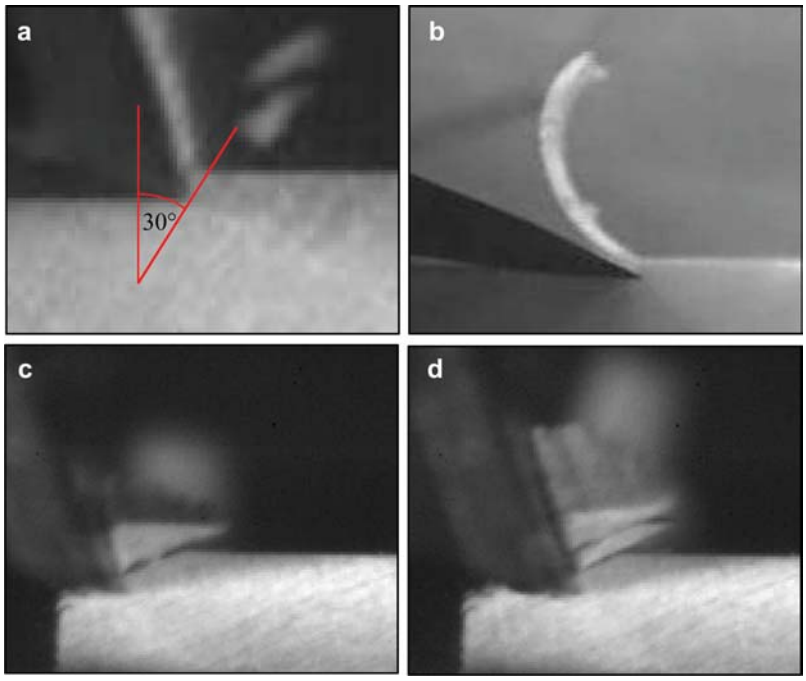

Figure 10 (a) Shear plane in line with grain. Douglas fir with 30° grain orientation. Processed at 0.2 mm DoC, 20° rake and 8 m s^{-1} cutting velocity. (b) Continuous chip formation. Douglas fir with 40° grain orientation. Processed at 0.4 mm DoC, 60° rake and 5 mm s^{-1} cutting velocity. (c–d) Discontinuous shear chip formation sequence (Douglas fir: 20° grain orientation, 0.6 mm DoC, 20° rake, 5 mm s^{-1} cutting velocity). (c) First chip sheared. (d) Second chip sheared and compression of wood prior to next shear.

The chip could be either continuous (as shown in Figure 10b) or discontinuous (Figures 10c, d), the latter illustrating the compression of the wood prior to shearing and the cyclic nature of the process.

A shear plane cutting theory proposed by Shaw et al. (1953) for metal cutting, where the shear plane is not on the plane of maximum stress, may be relevant to this shear plane chip formation mechanism. Due to the anisotropic properties of wood, the shear plane can be located in line with the grain, as the shear strength in that direction is lower than in other possible directions. Shaw et al. (1953) proposed that, for homogeneous materials, the shear plane was not on a plane of maximum stress due to interactions with friction on the tool rake face. Figure 11 shows a model similar to the Shaw et al. model for continuous chip formation but whereby the shear plane is in line with the orientation of the grain and the plane of maximum shear being offset by angle η. The stressed zone is contained within the borders ABC. The chip beyond BC is non-stressed, as is the workpiece material in front of the shear plane AC.

When machining at high speed with small DoC, it has been observed that this type of chip is propelled in line with the grain. Figure 12a illustrates some preliminary results obtained with a rake angle of 30° processing a specimen with a grain orientation of 30°. As can be seen

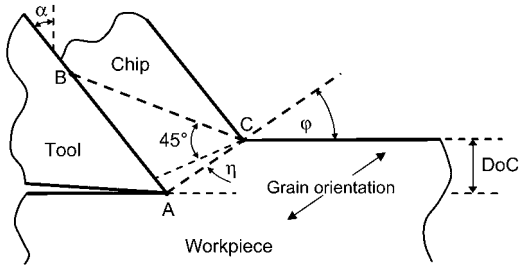

Figure 11 Proposed model for shear plane in line with grain orientation.

the chip is propelled along the grain and perpendicularly to the rake face. This phenomenon is observed for grain orientations almost perpendicular to the rake face. For other grain orientations it is not so apparent (Figure 12b) and the phenomenon also decreases with increasing the DoC.

Analysis of the chip formation according to classical McKenzie and Franz chip classification

Chips at 0° and 90° grain orientation

McKenzie (1961) identified two types of chip when cutting at a grain orientation of 90°. Confusingly, he used Roman numerals as Franz (1958) had done in his chip classification scheme, but the McKenzie type I and type II are *not* the same as the Franz type I and type II. The McKenzie type I and type II chips were both sub-categorised, indicated by the notation 'a' or 'b', with 'a' being a regular formation pattern and 'b' an irregular formation pattern. The McKenzie type I chips form with splits into the grain of the sample, type Ia having short regular splits and type Ib having several short splits between fairly regularly spaced longer splits; in type II the material not only fails in a plane perpendicular to the grain but also parallel to and below the tool path. Our experimental cuts, at both low and high speeds, performed at 90° grain orientation, replicated the McKenzie type Ia and type Ib chip formations, as shown in Figure 13a and b. Usually, the type Ia chip forms for lower depths of cut and the type Ib chip for higher depths of cut. The transition between the chip type Ia to chip type Ib has been observed going over 0.1 mm DoC when cutting at 5 mm s^{-1} and over 0.2 mm DoC when cutting a 8 m s^{-1}.

A McKenzie type IIb chip formation was observed either at slow or high speed experimental cutting at a 90° grain orientation. Figure 13c and d show the formation of a McKenzie type IIb chip when processing with high and low cutting speeds. The formation of the discontinuous chip (type b) occurs mainly in the earlywood.

No type IIa chips were observed at either slow or high speed at 90° grain orientation, but this type was observed at a 60° grain orientation (Figure 13e).

Franz (1958) classified three types of chip, all at zero grain orientation: type I is a chip formed by a split ahead of the tool and bending failure; type II is a chip formed by shear (the same process as the Merchant type 2 in metal cutting); and in type III, chips are formed by compression ahead of the tool. In our experiments, type I (Figure 13f) and type II chips (Figure 14) were found at 0° grain orientation, but no type III chips were found. Type I chip formation was found both at 8 m s^{-1} and 5 mm s^{-1} cutting velocities, with a 20° tool rake angle but with different DoC. When machining at 5 mm s^{-1} this type of chip was produced with DoC >0.2 mm, while with high speed cutting this type of chip was formed with DoC <0.1 mm. Type II as type I was also found at both velocities, but at different DoC (at 0.2 mm or lower at 5 mm s^{-1} and lower than 0.1 mm when cutting at 8 m s^{-1}). We believe that type III is more common when machining with very low or negative rake angles, lower than used in our cutting experiments; thus, this type of chip was not found in any of our experiments.

Chips formed at other grain orientations

The McKenzie type I chip formation (splits into the grain) were found in both high and low velocity cuts with negative grain orientations (i.e., cutting against the grain). However, the low velocity cuts performed with a 60° tool rake angle did not form the type I chip, whereas the low velocity cuts performed with a 20° tool rake angle did.

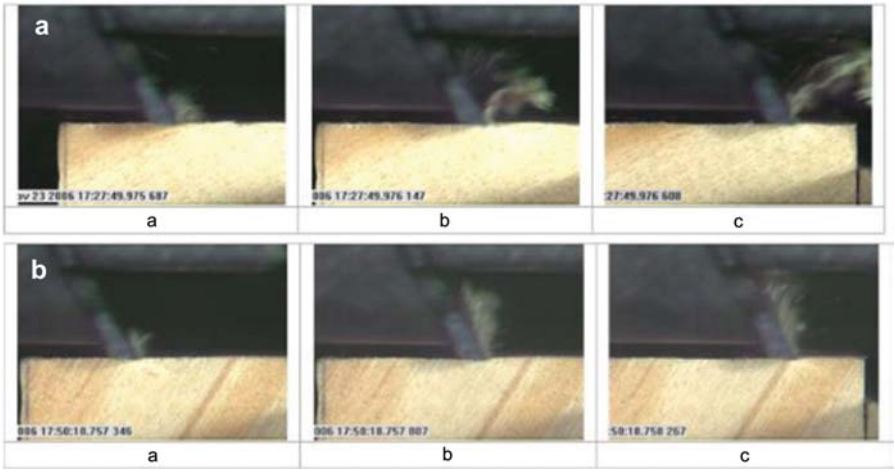

Figure 12 HSCR cutting sequences (a) Cutting with a rake angle of 30° and with 30° of grain orientation. (b) Cutting with a rake angle of 30° and 60° of grain orientation.

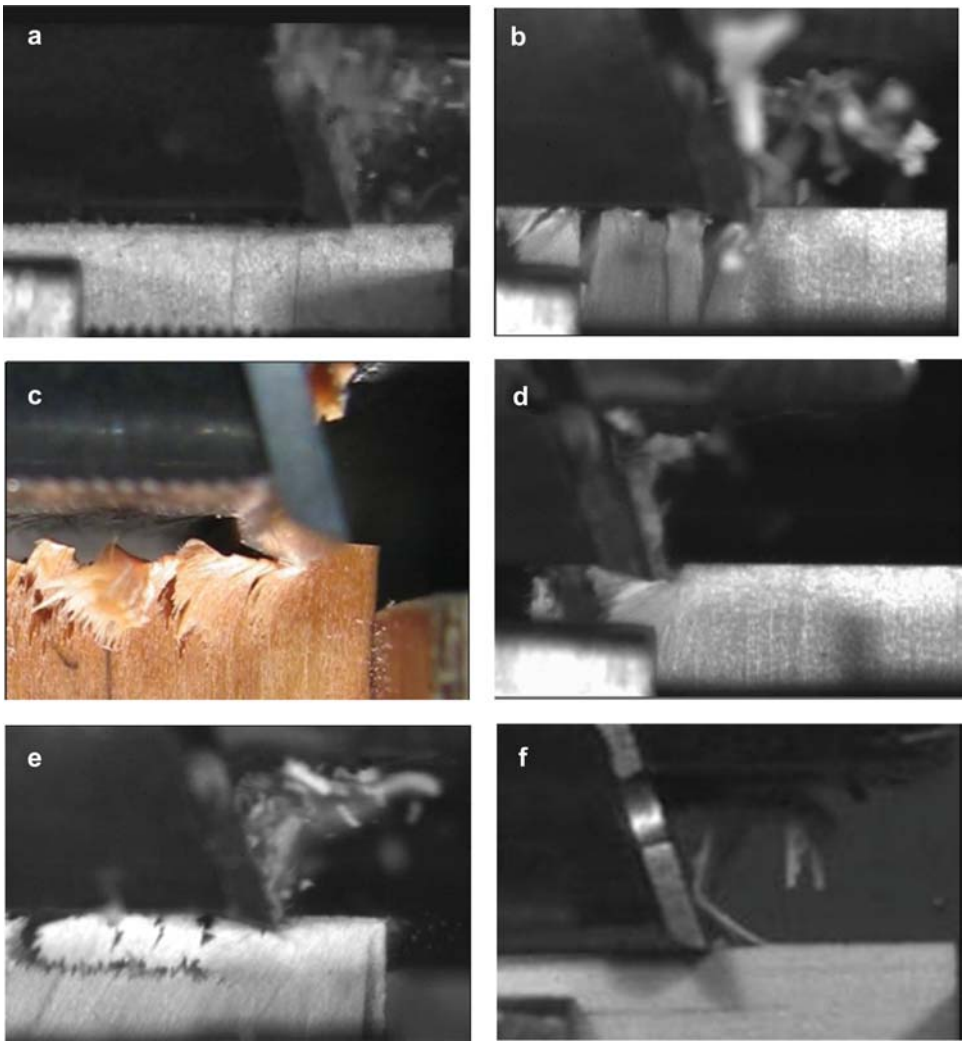

Figure 13 (a–e) McKenzie and (f) Franz chip formations processing Douglas fir. (a) Type Ia chip formation: 0.4 mm DoC, 5 mm s^{-1} cutting velocity, 20° tool rake angle, 90° grain orientation. (b) Type Ib chip formation: 0.6 mm DoC, 8 m s^{-1} cutting velocity, 20° tool rake angle, 90° grain orientation. (c) Type IIb chip formation: 0.6 mm DoC, 5 mm s^{-1} cutting velocity, 20° tool rake angle, 90° grain orientation. (d) Type IIb chip formation: 0.6 mm DoC, 8 m s^{-1} cutting velocity, 20° tool rake angle, 90° grain orientation. (e) Type IIa chip formation: 0.6 mm DoC, 8 m s^{-1} cutting velocity, 20° tool rake angle, 60° grain orientation. (f) Type I chip formation: 0.2 mm DoC, 8 m s^{-1} cutting velocity, 20° tool rake angle, 0° grain orientation.

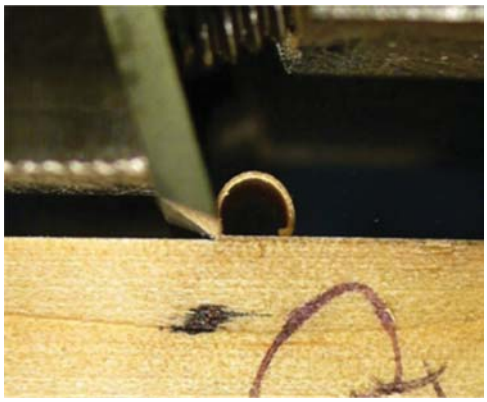

Figure 14 Franz type II chip formation. Douglas fir: 0.2 mm DoC, 5 mm s^{-1} cutting velocity, 20° tool rake angle, 0° grain orientation.

Only one low velocity cut at Florence (20° tool rake angle, 5 mm s^{-1} cutting velocity, -60° grain orientation and 0.2 mm DoC) produced a McKenzie type II chip (subsurface failure). However, McKenzie type II chips were observed at high speed at both negative and positive grain orientations. The subsurface failure occurred behind the tool tip. At negative grain orientations the failure was caused by grain rotation and tearing. At positive grain orientations the subsurface failure was caused by tool clearance face rubbing, which in turn caused subsurface tearing, predominantly in the earlywood. The Franz type I split-type chip was only observed at 0° grain orientation. Cutting performed on the instrumented microtome with the blade set at a 60° rake angle produced a Franz type II chip (shear type) at a -60° grain orientation with 0.2 mm DoC and at -70° grain orientation with a 0.4 mm DoC. Franz type II chips were not observed at negative grain orientations with the 20° rake angle at either high or low velocity. Table 2 shows a summary of the effects of tool rake angle, cutting velocity and depth of cut on the classic chip formations.

Effect of cutting speed on chip formation

Figure 15 combines chip types at different grain orientations, for both low and high cutting speeds, with iden-

Table 2 Summary of effect of parameters on the classic chip formations.

Type	Formation	Dependent upon		
		Rake angle	Velocity	Depth of cut
Franz type I	Splitting ahead of the tool tip	ΠΠ	ΠΠ	ΠΠ
Franz type II	Shear plane	ΠΠ	ΠΠ	ΠΠ
Franz type III	Compression	0	0	0
McKenzie type Ia	Regular splits into grain	ΠΠ	ΠΠ	ΠΠ
McKenzie type Ib	Irregular splits into grain	ΠΠ	ΠΠ	ΠΠ
McKenzie type IIa	Regular subsurface tearing	Π	ΠΠ	o
Positive grain	Caused by clearance face rubbing			
McKenzie type IIb	Irregular subsurface tearing	Π	ΠΠ	o
Positive grain	Caused by clearance face rubbing			
McKenzie type IIa	Regular subsurface tearing	Π	ΠΠ	o
Negative grain	Caused by grain rotation and tensile tearing			
McKenzie type IIb	Irregular subsurface tearing	Π	ΠΠ	o
Negative grain	Caused by grain rotation and tensile tearing			
New shear type	Shear plane in line with grain orientation	O	O	o

O = not dependant; Π = possible dependency; ΠΠ = definite dependency; 0 = chip type not found; o = not analysed/not clear.

tical tool geometries (rake angle $\alpha = 20°$ and DoC 0.2 mm).

The various types of chip produced at the different speeds at the same grain orientation are also shown. At 0°, the Franz chip is continuous at low speed (i.e., type II) but becomes the split-type at high speed (i.e., type I). At 90° grain orientation, the high speed chip disintegrates after formation. At other orientations, differences with speed may not be so marked. The differences in the chip formation for the other grain orientations will be the subject of other publications.

Modelling cutting forces

The forces to cut wood depend on wood species, density, MC, grain orientation, geometry, tool material and friction between chip and tool, and cutting speed. There are many empirical formulae for the variation in cutting force F_c with depth of cut t in wood processing (Kivimaa 1952; Kollmann and Côté 1968; Giordano 1981; Fischer 1989, 2004; Juan 1992; Eyma et al. 2004; Scholz and Troeger 2005). In a simple model, F_c depends directly on the cross-section being cut, i.e.,

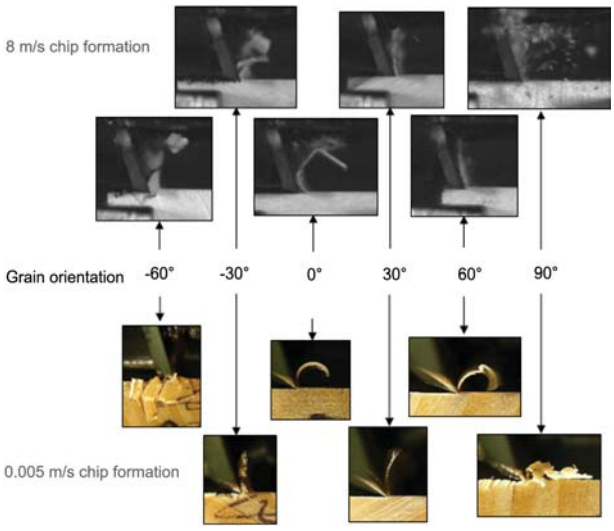

Figure 15 Varying chip types with grain orientation and cutting speed.

$$F_c = K_1\, w\, DoC \quad (1)$$

where K_1 is some constant and w is the width of cut (or kerf of a saw blade). Instead of a linear relation passing through the origin, another proposal is:

$$F_c = K_2\, w\, DoC^n \quad (2)$$

where K_2 is another constant and $n < 1$. Both the linear Eq. (1) and non-linear Eq. (2) have been generalised to include positive intercepts on the force axis, to give:

$$F_c = K_3 + K_4\, w\, DoC \quad (3)$$

and

$$F_c = K_5 + K_6\, w\, DoC^n \quad (4)$$

In addition, the momentum change of the chip has been included in analyses, as well as tool sharpness. Empirical relations for the power consumed in wood cutting may be obtained by multiplying the empirical expressions for force by the cutting velocity.

Relations, such as Eqs. (1)–(4), are obtained by curve-fitting experimental cutting force vs. DoC data.

The constants K relate specifically to the conditions of the experiments under which they were determined. They cannot be general, nor be extrapolated, because the well-known work of Franz (1958) demonstrates that depending principally on DoC and tool rake angle three types of chip may occur, namely continuous, discontinuous and a compression type of chip. It would appear that empirical curve fitting does not always recognise these differences, so that use and extrapolation of formulae for woods of different 'strength', or in conditions different from those under which data obtained, must be suspect. In order to provide a contribution to the development of new models to predict cutting forces in wood cutting, the Atkins theory (2003) has been applied to two classical cases of cutting: the formation of a Franz chip type II which will be called "offcut formation by shear" and the formation of a Franz chip type I which will be called "offcut formation by bending".

Offcut formation by shear

Continuum theories of cutting assume isotropic, homogeneous materials. Wood does not fulfil these criteria: it is highly anisotropic and compressibility of softwoods complicates the behaviour. Nevertheless, the Piispanen/Ernst-Merchant homogeneous isotropic theory is employed to predict machining forces for wood, sometimes incorporating variations in physical properties with direction.

The Piispanen/Ernst-Merchant model says that the chip is formed by shear on a well-defined plane emanating from the tip of the cutting edge to the free surface of the workpiece (Figure 11). In along-the-grain wood cutting, this type of chip is formed when the rake angle of the blade (with respect to the normal to the cut surface) is small, i.e., in saws.

Ernst-Merchant argued that cutting forces were determined solely by plasticity in the shear plane, and friction between chip and the rake face of the tool. To this day, there are great improvements in representation of the plastic flow field and friction, i.e., received wisdom in metal cutting. Atkins (2003) showed that significant work of separation (i.e., material fracture toughness) should be included in analyses of cutting. Work of surface separation in models of metal cutting was considered to be negligible because, when estimating its magnitude, the chemical surface free energy γ of a few J m^{-2} was employed rather than the fracture toughness of kJ m^{-2}, which modern ductile fracture mechanics would employ. Separation does not occur along a single plane as assumed in the definition of γ but rather is accompanied by boundary layers of irreversibility, so that specific works of separation R are approximately 1000$\times$ (free surface energy). Atkins (2003) showed that when separation work at the kJ m^{-2} level was incorporated in analyses for forces in cutting, many shortcomings of traditional analyses were removed. The component F_c of the cutting force in the direction of cutting is:

$$F_c = (kw\gamma_{shear}/Q_{shear})DoC + Rw/Q_{shear} = w\ DoC\ k(\gamma_{shear} + Z)/Q_{shear} \quad (5)$$

where the friction factor Q_{shear} is:

$$Q_{shear} = [1 - \{\sin\beta\ \sin\phi/\cos(\beta-\alpha)\cos(\phi-\alpha)\}] \quad (6)$$

and where the non-dimensional parameter Z is:

$$Z = R/k\ DoC \quad (7)$$

The component F_n of cutting force normal to the cut surface is:

$$F_n = F_c\tan(\beta-\alpha) \quad (8)$$

In the above equations, k is the shear yield stress, γ_{shear} is the shear strain along the shear plane inclined at angle ϕ, α is the rake angle of the tool (defined with respect to the normal to the cut surface), and β is the so-called angle of friction related to the coefficient of friction μ by $\mu = \tan\beta$. Eq. (5) without the second term incorporating R coincides with the traditional Ernst-Merchant theory. The shear strain is given by:

$$\gamma_{shear} = \cot\phi + \tan(\phi-\alpha) = \cos\alpha/\cos(\phi-\alpha)\sin\phi \quad (9)$$

and is unknown since the inclination ϕ of the shear plane is unknown. It is argued that ϕ is determined by minimising the work done or, equivalently, by minimising F_c. The closed-form solution for ϕ and hence F_c has recently been found by Williams (2008). He shows that:

$$\cot\phi = \tan(\beta-\alpha) \pm \sqrt{[1 + \tan^2(\beta-\alpha) + Z\{\tan(\beta-\alpha) + \tan\alpha\}]} \quad (10)$$

and hence:

$$F_c/Rw = (2/Z)\{\sqrt{[1 + \tan^2(\beta-\alpha) + Z\{\tan(\beta-\alpha) + \tan\alpha\}]} + \tan(\beta-\alpha)\} + 1 \quad (11)$$

Plots of (F_c/w) vs. DoC are therefore expected to have an intercept on the force axis equal in value to R. Furthermore, when $Z < 0.1$ (i.e., when $DoC > 10R/k$) ϕ and hence γ_{shear} are practically constant, making the coefficient of DoC constant, so that linear plots are expected. At smaller values of DoC, (F_c/w) vs. DoC curves down towards the origin but still has an intercept. It is clear that the empirical expressions, Eqs. (3) and (4), are all special versions of Eq. (11) applying to particular ranges of DoC. Use of Eqs. (1) and (2) would be in error at small depths of cut ['small' in relation to the length (R/k)]. Comparison of experimental wood cutting data and the above new theory has been successfully made (Wyeth and Atkins 2005; Atkins 2006).

It may be questioned why great advances have been made in metal cutting when a theory that ignores R is most often employed. It is because the thin boundary layers that form the top of the cut surface and the underside of the chip are so thin that the 'remote' flow field by which the offcut is formed is virtually independent of their existence. However, though having a small volume, the associated work per volume for separation is large, so that the contribution to total work and to the cutting forces is significant. Indeed, recent finite element method modelling of the transient start of orthogonal metal cutting (Rosa et al. 2007) shows that extremely fine meshes have to be employed to give sensible predictions for cutting forces.

Experimental evaluation of theory

Shear plane cutting tests were performed using the LSCR at the University of Reading. The Douglas fir test specimens were all of 0° grain orientation and the tool rake angle was set at 60°, this ensured that the chip formation process for each DoC was with a shear plane. The average cutting forces F_c (normalised by the width of the cut) vs. the DoC were plotted, as shown in Figure 16. A linear trend and a positive intercept was found as predicted by the proposed theory.

Offcut deformation by bending

In wood cutting, offcuts can form by bending when the rake angle of the tool is large, i.e., with the sort of knife-

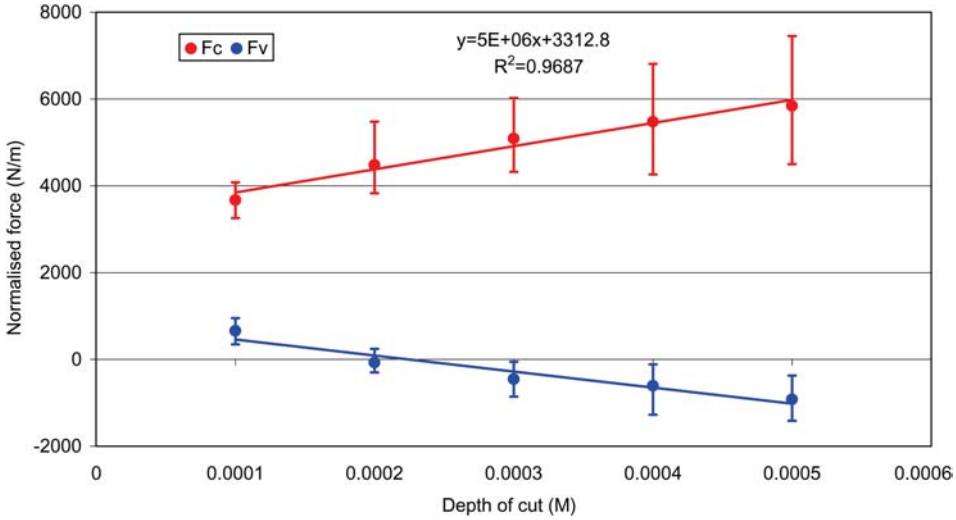

Figure 16 Plot of forces vs. depths of cut for 0° grain orientation samples, cut at low velocity and 60° tool rake angle.

like tools employed in veneer peeling (but most practical veneer peeling takes place with a 'nosebar' to avoid checking and this results in offcut formation by shear). Depending on the DoC and material properties, the offcut can remain elastic, or may be permanently curled up, as in wood planing. For elastic deformation:

$$F_c/Rw = 1/[1-\mu/\cos\theta(\sin\theta+\mu\cos\theta)] = 1/Q_{bend} \quad (12)$$

$$F_n/Rw = (1/\tan\theta) \quad (13)$$

where

$$Q_{bend} = [1-\mu/\cos\theta\ (\sin\theta+\mu\cos\theta)] \quad (14)$$

and where θ is the included angle of the wedge cutter so that, for small clearance angles, $\theta = (90-\alpha)°$. Note that the cutting force is constant, and the remarkable fact that F_n is independent of the friction.

For irreversible deformation of the offcut:

$$F_c/Rw = (1/Q_{bend})\{[\sqrt{(k\ DoC/R)}/2]+1\} = (1/Q_{bend})\{[\sqrt{(1/Z)}/2]+1\} \quad (15)$$

and

$$F_n = F_c\tan(\beta-\alpha) \quad (16)$$

with Q_{bend} as defined above. Hence, F_c varies as $\sqrt{DoC}$ with an intercept of Rw/Q_{bend} (Williams 1998).

Sometimes, it is difficult to be sure in which mode the chip is formed, i.e., in shear or in bending (Thibault 1988). The thrust force perpendicular to the cut surface is $F_n = F_c\tan(\beta-\alpha)$. When chips are formed in shear, F_n changes sign when $\alpha > \beta$ and also at sufficiently large *DoC* owing to the *Q* friction factor. When offcuts are formed in bending, the force on the beam has to remain in the same direction to provide the same sense bending moment at all times, so that F_n cannot change sign. Observation of the trends in F_n with *DoC* may help decide what sort of chip is forming. Analysis and comparison with experiments may be found in previously published work by Atkins (2006).

Conclusions

During the COST E35 action, research has been carried out in order to increase our knowledge of the chip formation process in orthogonal wood cutting with different grain orientations and DoC at low and high cutting speeds. Special devices have been developed. The same cutting geometry at each cutting speed has been used to compare the effect of velocity on the process. Complete test sets have been performed at both high and low cutting speed acquiring a large amount of data that still requires analysis and discussion. The work performed has enabled some progress in understanding the mechanics of chip formation and the factors that contribute to the forces and work required for cutting. The role of fracture toughness (crack resistance) is important, as well as 'strength' and friction between offcut and blade. A distinction has to be made as to how the chip is formed, namely in shear or by bending. The mathematical form of many empirical relations for cutting forces can now be given a scientific basis.

Owing to its anisotropy, wood remains a formidable material to model at all grain orientations. This is shown by the different, and complicated, types of chip that are formed at different grain orientations (and even at a single orientation, the type of chip may be different for different rake angles, different DoC, different frictional conditions and different cutting speeds). The study of chip formation, at low and high speeds over the whole range of grain orientations, described in this paper highlights the great variations that occur even for limited changes in rake angle and DoC.

A new chip classification has been proposed at some positive grain orientations. The shear plane was found to be in line with the grain orientation and not on the plane of maximum shear stress. This type of chip was found at both low and high cutting velocities and at both rake angles investigated. This chip type was found to be either

continuous (at low speed) or discontinuous (at high speed).

Acknowledgements

Much of the work reported in this paper was performed under the COST E35 programme of the European Science Foundation. Funding for Short Term Scientific Missions is gratefully acknowledged. D.J.W. thanks the UK Engineering and Physical Sciences Research Council for a research studentship. The EPSRC loan pool is thanked for the use of the high speed camera. We would like to acknowledge Prof. Andrea Del Taglia of the Faculty of Engineering of the University of Florence for lending the dynamometric platform which made possible the measurement of the cutting forces in Florence and Mr. Andrea Uccello who worked with us. Valuable discussions with Prof. George Jeronimidis at Reading and other participants in the COST action are gratefully acknowledged.

References

Atkins, A.G. (2003) Modelling metal cutting using modern ductile fracture mechanics: quantitative explanations for some longstanding problems. Int. J. Mech. Sci. 45:373–396.

Atkins, A.G. (2006) The role of fracture toughness in the cutting of wood. In: Proceedings of the 16th European Conference on Fracture, pp. 567–577, Andrianopoulos.

Costes, J.P., Ko, P.L., Ji, T., Decès-Petit, C. (2004) Orthogonal cutting mechanics of maple: modeling a solid wood-cutting process. J. Wood Sci. 50:28–34.

Cyra, G., Tanaka, C. (2000) The effects of wood-fiber directions on acoustic emission in routing. Wood Sci. Technol. 34: 237–252.

Eyma, F., Méausoone, P.J., Martin, P. (2004) Study of the properties of thirteen tropical wood species to improve the prediction of cutting forces in mode B. Ann. Forest Sci. 61: 55–64.

Fischer, R. (1989) Konzept für ein Modell der spanenden Bearbeitung von Holzwerkstoffen. Wissenshaftliche Zeitschrift der TU Dresden 38-2.

Fischer, R. (2004) Micro processes at cutting edge – some basics of machining wood. In: Proceedings of the 2nd International Symposium on Wood Machining, Vienna, Austria. pp. 191–202.

Franz, N.C. An Analysis of the Wood-cutting Process. The University of Michigan Press, Ann Arbor 1958.

Giordano, G. (1981) Tecnologia del legno. Unione Tipografico-Editrice Torinese.

Goli, G., Bleron, L., Marchal, R., Uzielli, L., Negri, M. (2002) Surfaces formation and quality, in moulding wood at various grain angles. Initial results with Douglas fir and oak. In: Wood Structure and Properties Proceedings, Brezno, Slovakia. pp. 91–98.

Goli, G., Uzielli, L. (2004) Mechanisms of wood surface formation and resulting final condition after planing. In: Proceedings of the 2nd International Symposium on Wood Machining, Vienna, Austria. pp. 451–457.

Goli, G., Marchal, R., Uzielli, L. (2004) Classification of wood surface defects according to their mechanical formation during machining. In: Proceedings of the 2nd International Symposium on Wood Machining, Vienna, Austria. pp. 315–324.

Goli, G., Fioravanti, M., Sodini, N., Jiangang, Z., Uzielli, L. (2005) Wood processing: a contribution to the interpretation of surface origin according to grain orientation. In: Proceedings of the 17th IWMS, Rosenheim, Germany, pp. 44–54.

Goli, G., Fioravanti, M., Del Taglia, A. (2006) Chip formation processing wood with different grain orientations using low speed free orthogonal cutting technique. In: Proceedings of the Conference "Integrated Approach to Wood Structure, Behaviour and Applications", joint meeting of the European Society for Wood Mechanics and COST E35, Florence, Italy. pp. 291–300.

Goli, G., Wyeth, D., Atkins, A.G., Jeronimidis, G., Fioravanti, M. (2007a) Orthogonal cutting of wood at high speed using a modified split Hopkinson Bar and a high speed camera. In: 3rd International Symposium on Wood Machining, Lausanne, Switzerland. pp. 35–38.

Goli, G., Wyeth, D., Atkins, A.G., Jeronimidis, G., Fioravanti, M., Del Taglia, A. (2007b) Chip formation in wood cutting with different grain orientations using high and low cutting speeds. In: Proceedings of the 8th Associazione Italiana di Tecnologia Meccanica conference, Montecatini, Italy. pp. 57–58.

Juan, J. (1992) Comment bien usiner le bois. Centre Technique du Bois et de l'Ameublement.

Kivimaa, E. (1952) Die Schnittkraft in der Holzbeareitung. Holz Roh Werk. 10:94–108.

Kollmann, F.F.P., Côté, W.A. Jr. Principles of Wood Science and Technology. Springer-Verlag, New York, 1968.

McKenzie, W.M. (1961) Fundamental analysis of the wood-cutting process. PhD thesis, University of Michigan, MI, USA.

McLauchlan, T.A., Lapointe, J.A. (1979) Production of chips by disc chippers. In: Pulp and Paper Technology Series, No. 5, Chip Quality Monograph, Ed. Hatton, J.V. pp. 15–32.

Rosa, P.A.R., Martins, P.A.F., Atkins, A.G. (2007) The transient beginning to machining and the transition to steady-state cutting. Int. J. Mach. Tools Manufact. 47:1904–1915.

Scholz, F., Troeger, J. (2005) Modelling of cutting forces. In: Proceedings of the 17th IWMS, Rosenheim, International Wood Machining Seminar, pp. 260–264.

Shaw, M.C., Cook, N.H., Finnie, I. (1953) The shear angle relationship in metal cutting. Trans. ASME 75:273–288.

Stewart, H.A. (1971) Chip formation when orthogonally cutting wood against the grain. Wood Sci. 3:193–203.

Stewart, H.A. (1983) A model for predicting wood failure with respect to grain angle in orthogonal cutting. Wood Fiber Sci. 15:317–325.

Thibau, B. (1988) Le processus de coupe du bois par deroulage. PhD dissertation. Université des Sciences et Techniques du Languedoc, Montpellier, France.

Williams, J.G. (1998) Friction and plasticity effects in wedge splitting and cutting fracture tests. J. Materials Sci. 33: 5351–5357.

Williams, J.G. (2008) Personal communication.

Wyeth, D.J., Atkins, A.G. (2005) Cutting forces for wood determined on an instrumented sledge microtome. In: Proceedings of COST Action E-35, University of Technology, Lapeenranta, Finland. pp. 101–110.

Wyeth, D., Goli, G., Atkins, A.G., Jeronimidis, G., Fioravanti, M. (2007) Friction in orthogonal cutting of Douglas fir at varying grain orientations: measurements and consequences. In: 3rd International Symposium on Wood Machining, Lausanne, Switzerland. pp. 139–142.

Received April 4, 2008. Accepted October 23, 2008.
Previously published online November 28, 2008.